Paper presented at INTER-NOISE 2021 Washington, DC, August 01-05 2021
Version of record: https://doi.org/10.3397/IN-2021-2334

Influence of mobility completeness and source behavior on the robustness of Component-Based Transfer Path Analysis methods: A numerical study.

Simon Prenant[1],
Thomas Padois,
Thomas Dupont,
Olivier Doutres
Department of Mechanical Engineering, École de technologie supérieure, 1100 rue Notre-Dame Ouest, Montréal, Québec, H3C 1K3, Canada

ABSTRACT

Structure borne noise (SBN) is considered as a major contribution to the noise generated inside aircrafts. Engineering methods, such as Component-Based Transfer Path Analysis (CB-TPA) methods, have been developed for SBN assessment. These methods are based on active and passive properties of the source and the receiving structure being coupled or decoupled. The theoretical formulation requires mobility according to all Degrees Of Freedom (DOFs) but the rotational DOFs cannot be measured easily. To this end, indirect methods have been developed and specific sensors have been proposed, resulting in a more complex experimental set-up and an increase in measurement uncertainties. The need for assessing the full mobility matrices thus deserves to be investigated. The robustness of these methods with respect to the matrix completeness and the source behavior is investigated numerically in this work. A numerical model has been developed to simulate vibrating sources with simple or complex vibratory behavior and to assess the mobility matrices for any completenesses. Velocity on the receiving structure is used as a target indicator. The influence of the source behavior and matrix completeness are discussed, and the results show that the required mobility matrix completeness depends on the source behavior.

1. INTRODUCTION

Aircraft and helicopter manufacturers are interested in mastering the Structure Borne Noise (SBN) generated in the cabins and which originates from embedded vibrating systems [1]. Promising methods such as the Component-based Transfer Path Analysis (CB-TPA) methods could be used from the early phase of development for predicting SBN, but also during the validation phase. The CB-TPA methods require the knowledge of the intrinsic active dynamic property of the vibrating system (i.e., equivalent force at the connection points) and the passive property of the coupled structure (i.e., mobility matrix) [2]. The latter could also be estimated form the passive property of the decoupled components using a Dynamic Substructuring (DS) procedure [3]. The joint use of CB-TPA and DS, referred to as CB-TPA-DS hereafter, is thus well suited for the design phase when the two components are in development and cannot yet be coupled in practice. However, the application of CB-TPA methods is experimentally challenging [4] since the structure mobility assessment requires the 36 terms of the matrix when both translational and rotational degrees of freedom (DOF) are considered [5]. The

[1] simon.prenant.1@ens.etsmtl.ca

terms of the mobility matrix related to rotational degrees of freedom (RDOFs) represent 75% of the matrix completeness and are often neglected to reduce the measurement effort. Numerical investigations [6]–[8] have demonstrated that RDOFs cannot be neglected during DS procedure. Assessing the RDOF terms of the mobility matrix is feasible but requires indirect methods [5], [9] or specific instrumentation [10]. It has been suggested that the benefit of including RDOFs for CB-TPA application depends on the dynamic behavior of the components [11], the used method [12] and the quality of the RDOFs determination [13]. Past investigations on the impact of RDOFs omission generally consist in comparing a matrix completeness involving all DOFs to one involving only translational DOFs (TDOFs) and do not consider the possible influence of the system active behavior. In contrast, the impact of omitting the terms related to in-plane DOFs is not well known [14]. In this paper, the effect of the mobility matrix incompleteness on the accuracy of CB-TPA and CB-TPA-DS methods is addressed through a numerical study. This study is carried out on coupled structure made of a clamped aluminum plate and a cubic source having two different vibrating active behaviors.
Four mobility matrix completenesses are considered and involve different measurement efforts and technique capabilities. Section 2 starts with the theoretical background on the CB-TPA and CB-TPA-DS methods. Section 3 presents the numerical model. The results are shown and discussed in Section 4.

2. Theoretical background

CB-TPA and CB-TPA-DS methods allow assessing the dynamical response of a coupled structure *AB* at a target point (3), as seen on Figure 1. The coupled structure is made of a vibrating source *A* attached to a receiving structure *B*. Both components are connected together at interface (2) through a rigid and massless connection. The physical indicator at the target location (3) could be a movement quantity such as velocity u_3.
The CB-TPA method requires the transfer mobility of the coupled structure $\mathbf{Y}_{32}^{AB}$ and the equivalent force (also called blocked force) of the source f_2^{eq} at the connection point to give the target velocity u_3 according to (see the step a) and b1) in Figure 1)

$$u_3 = \mathbf{Y}_{32}^{AB} f_2^{eq}. \tag{1}$$

f_2^{eq} are assessed *in situ* using an indirect approach requiring the transfer mobility $\mathbf{Y}_{42}^{AB}$ and the velocity u_4 (see the step a) in Figure 1) according to

$$f_2^{eq} = (\mathbf{Y}_{42}^{AB})^{+} u_4. \tag{2}$$

In the following, the CB-TPA method based on Eqs. (1) and (2) is referred to as CB-TPA-IS. For assessing the target response u_3 based only on decoupled component properties, a DS procedure (see the step b2) in Figure 1) is used to reconstruct the transfer mobility of the coupled structure $\mathbf{Y}_{32}^{AB}$ based on the mobility matrices of the decoupled components $\mathbf{Y}_{22}^{A}$, $\mathbf{Y}_{22}^{B}$ and $\mathbf{Y}_{32}^{B}$ according to

$$\mathbf{Y}_{32}^{AB} = \mathbf{Y}_{32}^{B}(\mathbf{Y}_{22}^{A} + \mathbf{Y}_{22}^{B})^{-1}\mathbf{Y}_{22}^{A}. \tag{3}$$

The CB-TPA method based on Eqs. (1) and (3) (i.e., involving DS procedure) is referred to as CB-TPA-DS-IS in the following.

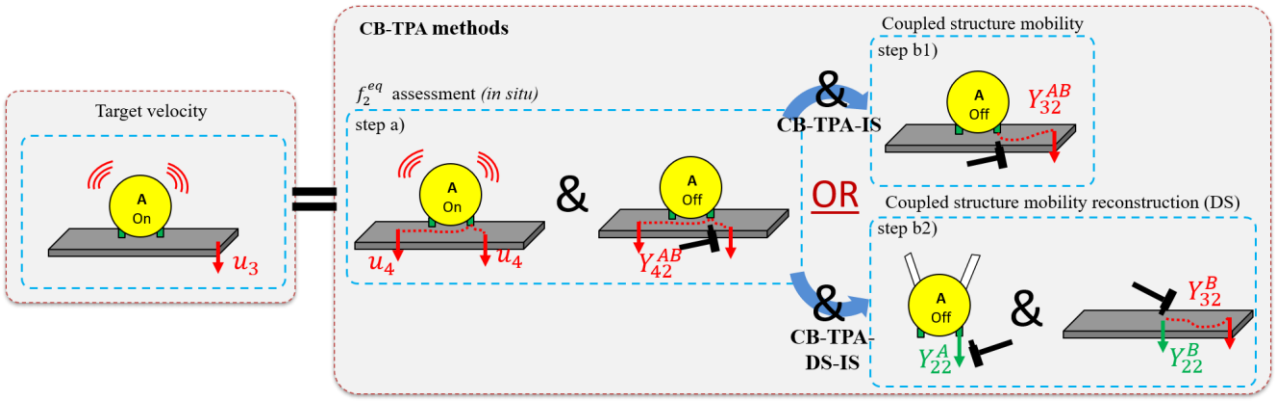

Figure 1 : Schematic representation of the steps involved in the application of the CB-TPA (steps a) and b)) and CB-TPA-DS-IS (steps a) and c)) methods.

The CB-TPA-IS and CB-TPA-IS-DS methods are used to assess the target velocity at numerous point locations uniformly distributed on an area S of the receiving structure. The spatial averaged mean-square velocity $\langle u_3^2 \rangle$ is then computed according to

$$\langle u_3^2 \rangle = \frac{1}{2S} \iint_S |u_3(x,y)|^2 dS, \tag{4}$$

where u_3 is the component of the target velocity normal to the surface of the structure. The mean-square velocity $\langle u_3^2 \rangle$ is used here as an objective indicator for evaluating the impact of matrices incompleteness on the accuracy of the CB-TPA methods. Only the velocity normal to the surface of the receiving structure is considered.

3. Numerical model

3.1. Source, receiving structure, test bench and coupled structure

The numerical model has been developed with Ansys Mechanical APDL. Components and coupled structure geometries are presented in Figure 2. An aluminum cubic 100 mm square in shape is used as the source. The geometry is meshed with 20 000 solid elements with 6 DOFs/node. The active dynamic behavior of the source is modeled by applying excitations to the faces of the cube as detailed in Section 3.2. Here, the receiving structure is an aluminum plate whose dimensions are (1371.6×965.2×3 mm^3) and the plate boundary conditions are clamped. The geometry is meshed with 14 000 shell elements with 6 DOFs/node. Using a plate is a common practice to mimic in a simple way the dynamic behavior of an aircraft structure [1].

Components are rigidly coupled together thanks the Multi Point Constraints (MPC) method. The mechanical properties of the aluminum of both components are: Young's modulus of 65.6 GPa, density of 2700 kg/m^3, Poisson's ratio of 0.33 and damping of 5%.

The simulations have been performed using a complete resolution (i.e., without modal summation) with a frequency step of 1 Hz over a frequency range from 40 to 3000 Hz.

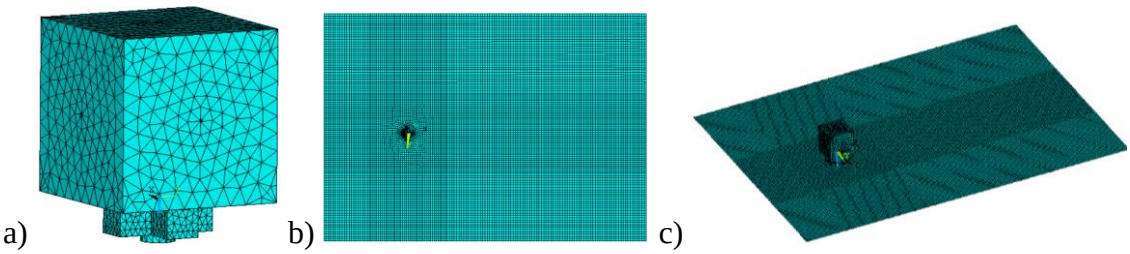

Figure 2 : Meshes geometries of the a) source, b) receiving structure and c) coupled structure.

3.2. Source excitation

Two different active dynamic behaviors have been simulated and are referred to as Excitation#1 and Excitation#2. The amplitude and location of force and moment components of the two sources are given in Figure 3. Pilot nodes have been used to apply moments.

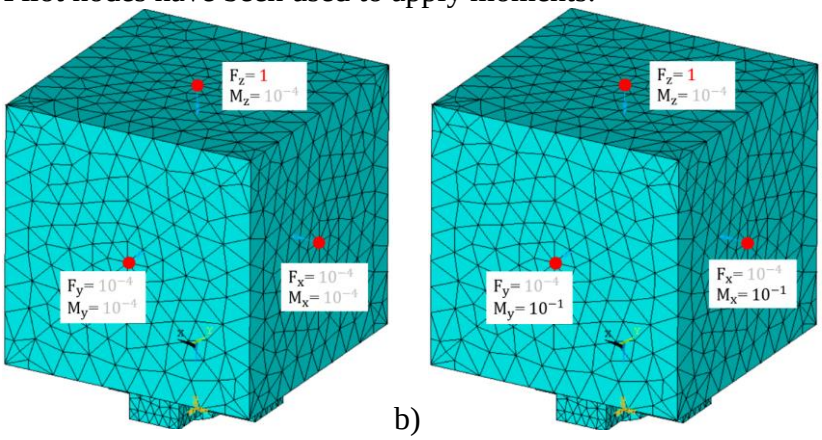

a) b)

Figure 3 : Details of the set of excitations applied for the a) Excitation#1 and b) Excitation#2.

Excitation#1 is considered as the source with the simple active dynamic behavior, mainly in translation along the Z-axis. Excitation#2 is more complex since it generates a force along z and two moments around x and y axes.

3.3. Mobility matrix completeness

The following four mobility matrix completenesses are considered for investigations:

- The FULL completeness, which includes the 6 DOFs (i.e., $\mathbf{Y}_{22}^{A}$, $\mathbf{Y}_{22}^{B}$ and $\mathbf{Y}_{22}^{AB} \in \mathbb{C}^{6x6}$).
- The OOP completeness, which includes the 3 out-of-plane DOFs (i.e., $\mathbf{Y}_{22}^{A}$, $\mathbf{Y}_{22}^{B}$ and $\mathbf{Y}_{22}^{AB} \in \mathbb{C}^{3x3}$), namely the Z-axis TDOF and the X- and Y-axis RDOFs. This completeness is well suited for bending motions.
- The TDOF completeness, which includes the 3 TODFs (i.e., $\mathbf{Y}_{22}^{A}$, $\mathbf{Y}_{22}^{B}$ and $\mathbf{Y}_{22}^{AB} \in \mathbb{C}^{3x3}$).
- The Z completeness, which includes the Z-axis TODF only (i.e., $\mathbf{Y}_{22}^{A}$, $\mathbf{Y}_{22}^{B}$ and $\mathbf{Y}_{22}^{AB} \in \mathbb{C}^{1x1}$).

A depiction of the four mobility matrix completenesses is shown in Figure 4. The TDOF and Z completeness require only an impact hammer and accelerometers for experimental application, while the FULL and OOP require specific instrumentation or indirect methods to assess terms related to RDOFs, inducing additional sources of uncertainties.

	F_X	F_Y	F_Z	M_X	M_Y	M_Z
u_X	$Y_{u_X F_X}$	$Y_{u_X F_Y}$	$Y_{u_X F_Z}$	$Y_{u_X M_X}$	$Y_{u_X M_Y}$	$Y_{u_X M_Z}$
u_Y	$Y_{u_Y F_X}$	$Y_{u_Y F_Y}$	$Y_{u_Y F_Z}$	$Y_{u_Y M_X}$	$Y_{u_Y M_Y}$	$Y_{u_Y M_Z}$
u_Z	$Y_{u_Z F_X}$	$Y_{u_Z F_Y}$	$Y_{u_Z F_Z}$	$Y_{u_Z M_X}$	$Y_{u_Z M_Y}$	$Y_{u_Z M_Z}$
θ_X	$Y_{\theta_X F_X}$	$Y_{\theta_X F_Y}$	$Y_{\theta_X F_Z}$	$Y_{\theta_X M_X}$	$Y_{\theta_X M_Y}$	$Y_{\theta_X M_Z}$
θ_Y	$Y_{\theta_Y F_X}$	$Y_{\theta_Y F_Y}$	$Y_{\theta_Y F_Z}$	$Y_{\theta_Y M_X}$	$Y_{\theta_Y M_Y}$	$Y_{\theta_Y M_Z}$
θ_Z	$Y_{\theta_Z F_X}$	$Y_{\theta_Z F_Y}$	$Y_{\theta_Z F_Z}$	$Y_{\theta_Z M_X}$	$Y_{\theta_Z M_Y}$	$Y_{\theta_Z M_Z}$

Completeness: Z TDOF OOP FULL

Figure 4 : Depiction of the Z, TDOF, OOP and FULL completenesses considered (color online).

4. Results and discussion

4.1. Description of the boxplot representation

This section first investigates the accuracy of the CB-TPA-IS method (Eq. (1) and (2)) when the second source (Excitation#2) is considered. A direct comparison of the reference and assessed target

mean-square velocity $\langle u_3^2 \rangle$ is shown in Figure 5. The reference and assessed target $\langle u_3^2 \rangle$ spectra when the FULL completeness is considered are shown in Figure 5 a) and b), respectively in narrow band and 12th octave band. The target $\langle u_3^2 \rangle$ is perfectly assessed when the FULL completeness is considered, which allows verifying the application of the CB-TPA method. The reference and assessed target $\langle u_3^2 \rangle$ spectra when the Z completeness is considered are shown in Figure 5 c) and d) respectively in narrow band and 12th octave band. The target $\langle u_3^2 \rangle$ is globally correctly assessed but large discrepancies appear at low and high frequencies.

For synthesis purposes, a statistical tool is proposed for rapidly evaluating the accuracy of the target dynamic behavior assessment. To this end, the difference between the assessed and reference target $\langle u_3^2 \rangle$ is first computed at each frequency, then, averaged over the frequency range of interest and finally, statistical quantities (e.g., mean, median, quartiles) are calculated and represented using a boxplot. The boxplots associated to Figure 5 a) and b) and c) and d) are respectively shown in Figure 5 e) and f). The red line and black cross correspond respectively to the median and mean value and allows quantifying the trend/accuracy of a method (i.e., if it is globally over- or under-estimating the target response). Two medians are considered to be different when the notches of the associated boxes do not overlap. The blue box limits the 1st and 3rd quartiles, namely 50% of the values are included inside, and is called Interquartile Range (IQR). The box is extended by whiskers that have a maximum length of 1.5 times the IQR. The box and the whiskers allow for quantifying the variability of the target assessment over the frequency range of interest. The red crosses represent the outliers and are considered as statistically different from the others (i.e., which are associated with local phenomena).

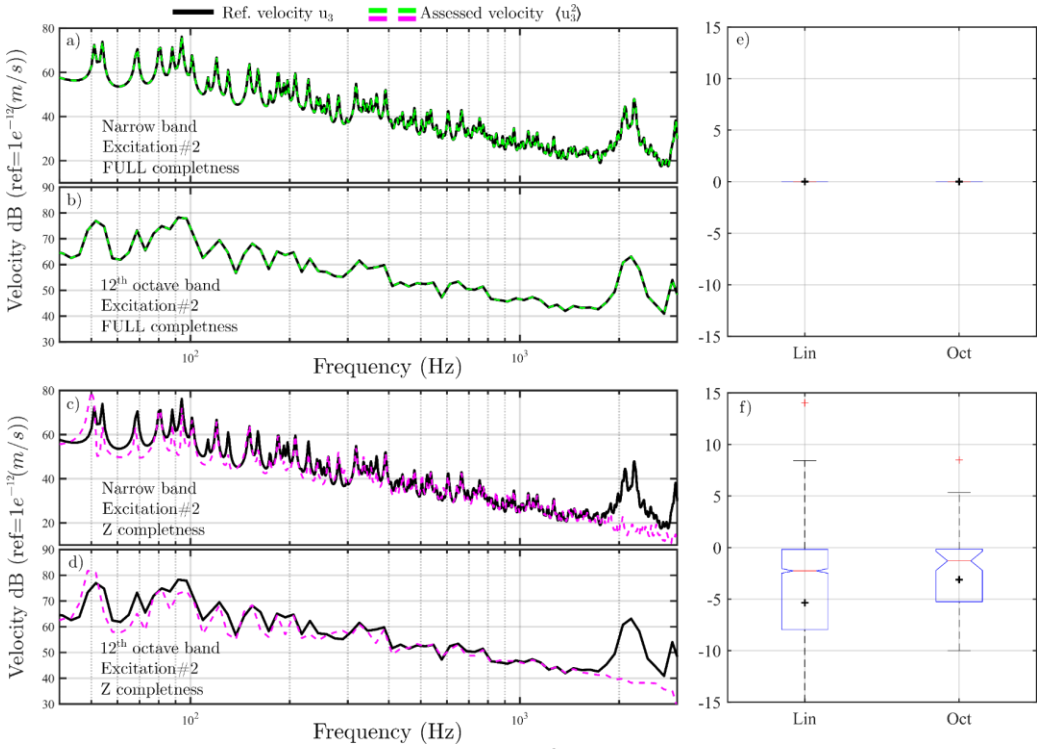

Figure 5 : Reference and assessed target indicator $\langle u_3^2 \rangle$ using the CB-TPA-IS method: in a) narrow and b) 12th octave band considering FULL completeness and in c) narrow and d) 12th octave band considering Z completeness. Boxplot representation of the difference between the reference and assessed target indicator $\langle u_3^2 \rangle$ associated to e) the FULL and f) the Z completenesses.

For both FULL and Z completenesses, the 12th octave band allows to keep the overall and local trends of the narrow band representation while smoothing the curve a bit. This smoothing allows to reduce the number of outliers in the boxplot and therefore to have a better understanding of the content of the boxplot. For the following, only the boxplots associated to the 12th octave band are considered, increasing the influence of low frequencies in the boxplot representations, since the octaves are smaller at low frequencies.

4.2. Transfer path analysis methods robustness evaluation

The target indicator $\langle u_3^2 \rangle$ is assessed using each CB-TPA method, source excitation and mobility matrix completeness and is shown in Figure 6 using the boxplot representation.

As shown in Figure 6 a), the CB-TPA-IS method correctly assesses the target vibratory indicator of the plate $\langle u_3^2 \rangle$ when Excitation#1 is considered (see green part of Figure 6 a)), regardless the completeness. This result suggests that, as expected, the simple source configuration only involves the contribution of the Z-axis TDOF which is the most significant. A mobility matrix completeness including 1 or 3 TDOFs could be suitable when sources with simple active dynamic behavior are considered. However, when a source with a more complex active dynamic behavior is considered such as Excitation#2 (see red part of Figure 6 a)), only the FULL and OOP completenesses allow a perfect assessment of the target indicator. In this case, the passive dynamic behavior of the coupled structure is mainly governed by bending. The TDOF and Z completenesses are not well suited for describing bending motions. In this case, the OOP completeness seems to be the best trade-off between robustness and ease of application since it does not require the measurement of in-plane terms, often difficult to measure experimentally.

As shown in Figure 6 b), the CB-TPA-DS-IS method is less accurate than the CB-TPA-IS method. When Excitation#1 is considered (see green part of Figure 6 b)), $\langle u_3^2 \rangle$ is perfectly assessed with FULL completeness and is satisfyingly estimated with the other completenesses. When Excitation#2 is considered (see red part of Figure 6 b)), $\langle u_3^2 \rangle$ is perfectly assessed with FULL completeness and the three other completenesses lead to inconsistent assessments, especially for the OOP completeness. These inaccuracies are most probably due to the reconstruction of $\mathbf{Y}_{32}^{AB}$ by the DS procedure, based on the components mobilities, since the f_2^{eq} are the same than those previously used in the CB-TPA-IS method. The terms with the highest amplitude of $\mathbf{Y}_{22}^{A}$ are located on the diagonal and an anti-diagonal of the mobility matrix, while the receiving structure mobilities $\mathbf{Y}_{22}^{B}$ and $\mathbf{Y}_{32}^{B}$ are mainly governed by bending (i.e., terms related to the out-of-plan DOFs). Only the FULL completeness allows to correctly reconstruct $\mathbf{Y}_{32}^{AB}$. The reconstruction of this mobility therefore seems to be a very sensitive process. When components with different passive dynamic behavior are considered, it is suggested to consider all of the DOFs, in order to provide a good reconstruction of the coupled structure mobility. These inaccuracies may be amplified when sources with complex active dynamic behavior is involved.

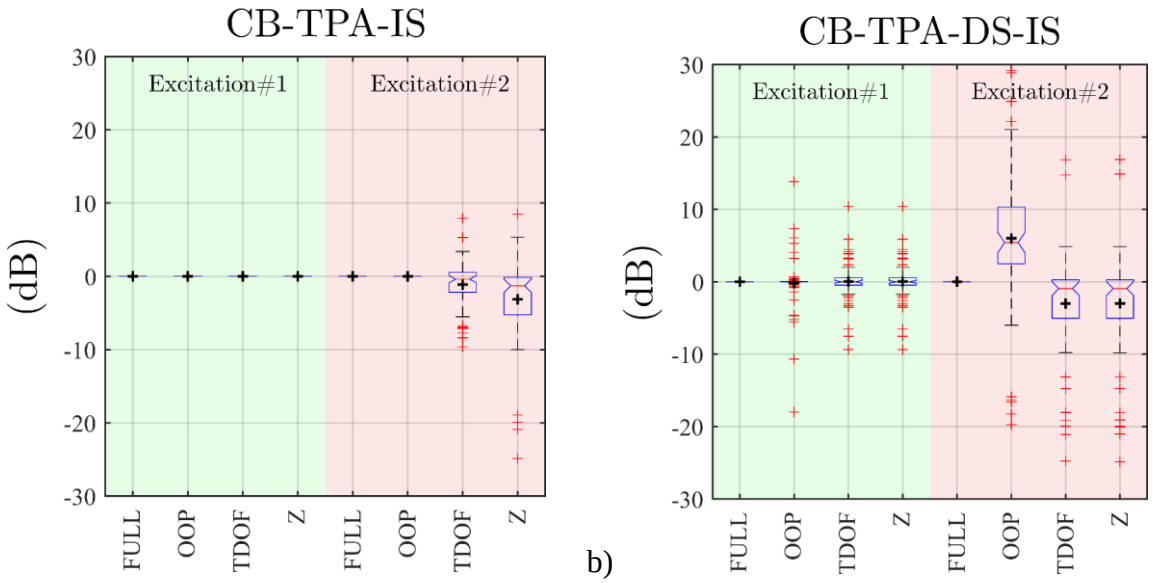

Figure 6 : Boxplots representation related to the a) CB-TPA-IS and b) CB-TPA-DS-IS methods, considering the four completenesses and excitations.

5. CONCLUSIONS

The CB-TPA with or without DS are promising methods for controlling noise on aircraft, but are still limited by experimental challenges such as the selection of DOFs required to fill in the mobility matrices. In this work, the influence of mobility matrix incompleteness on the CB-TPA-IS and CB-TPA-DS-IS methods has been addressed, considering two distinct active dynamic behaviors of the source and four mobility matrix completenesses. The spatial averaged mean-square velocity of the receiving structure has been determined from the aforementioned CB-TPA methods and used as objective indicator to evaluate their accuracy.

It has been observed that the influence of the mobility matrix completeness depends on the CB-TPA method (i.e., with or without DS) and on the complexity of the active dynamic behavior of the source. The CB-TPA-IS method provides good velocity assessments, if not perfect, regardless the source active dynamic behavior when the OOP completeness is considered. Indeed, this completeness is well suited for characterizing the bending behavior of the coupled structure. The CB-TPA-DS-IS method is based only on decoupled properties of the assembly and is shown to be less accurate than the CB-TPA-IS method. The reconstruction of the coupled structure mobility by the DS procedure seems to be very sensitive to the matrix completeness. For this reason, a FULL completeness seems to be the only suitable one, especially when a source with a complex active dynamic behavior is considered. As perspectives, the investigations on the robustness of the CB-TPA methods could be extended 1) by considering other CB-TPA methods, 2) by evaluating other sources of uncertainties and 3) by validating/completing the observations with experimental applications.

6. ACKNOWLEDGEMENTS

This work has been supported by (alphabetically ordering) Bell Helicopter Textron Canada, Bombardier Aerospace, CRIAQ (Consortium for Research and Innovation in Aerospace in Canada), NSERC (Natural Sciences and Engineering Research Council of Canada) and Parker Hannifin Corporation.

7. REFERENCES

[1] Fiorentin, T. A., Ferguson, N. S., Renno, J. M., and Lenzi, A. Structural response of an aircraft fuselage to hydraulic system-A wave and mobility approach. *Noise Control Engineering Journal*, 2013, vol. **61**, no 1, p.87-99.

[2] van der Seijs, M. V., de Klerk, D., and Rixen, D. J., General framework for transfer path analysis: History, theory and classification of techniques, *Mechanical Systems and Signal Processing*, 2016, vol. **68**, p.217-244.

[3] de Klerk, D., Rixen, D. J., and Voormeeren, S. N., General framework for dynamic substructuring: history, review and classification of techniques. *AIAA journal*, 2008, vol. **46**, no 5, p. 1169-1181.

[4] Allen, M. S., Rixen, D., Van der Seijs, M., Tiso, P., Abrahamsson, T., and Mayes, R. L., Substructuring in Engineering Dynamics, *Springer International Publishing*, 2020.

[5] de Klerk, D., Rixen, D., Voormeeren, S. N., and Pasteuning, F. Solving the RDoF problem in experimental dynamic substructuring. *Proceedings of the Twentysixth International Modal Analysis Conference*, Orlando, FL. 2008.

[6] Duarte, M. L. M. et Ewins, D. J., Some insights into the importance of rotational degrees-of-freedom and residual terms in coupled structure analysis. *Proceeding of the international society for optical engineering*. Spie International Society for Optical, 1995. p. 164 - 170.

[7] Gialamas, T., Tsahalis, D., Bregant, L., et al., Substructuring by means of FRFs: some investigations on the signifcance of rotational DOFs. *Proceeding of the international society for optical engineering*. Spie International Society for Optical, 1996. p. 619 - 625.

[8] Liu, W. et Ewins, D., The importance assessment of RDOF in FRF coupling analysis. *Proceedings of the Seventeenth International Modal Analysis Conference*. 1999. p. 1481-1487.

[9] Duarte, M. L. M., and Ewins, D. J., Rotational degrees of freedom for structural coupling analysis via finite-difference technique with residual compensation. *Mechanical Systems and Signal Processing*, 2000, vol. **14**, no 2, p. 205-227.

[10] Drozg, A., Rogelj, J., Cepon, G., and Boltezar, M., On the performance of direct piezoelectric rotational accelerometers in experimental structural dynamics. *Measurement*, 2018, vol. **127**, p. 292-298.

[11] Campbell, R. L. et Hambric, S. A., Application of Frequency Domain Substructure Synthesis Technique for Plates loaded with Complex Attachments. Pennsylvania State University Park applied research Lab, 2004.

[12] Elliott, A. S., Moorhouse, A. T., Huntley, T., et al., In-situ source path contribution analysis of structure borne road noise. *Journal of Sound and Vibration*, 2013, vol. **332**, no 24, p. 6276-6295.

[13] Helderweirt, S., van der Auweraer, H., Mas, P., et al., Application of accelerometer-based rotational degree of freedom measurements for engine subframe modelling. *Proceeding of IMAC-XIX: A Conference on Structural Dynamics*, 2001. p. 1298-1304.
[14] Elliott, A., Moorhouse, A., Meggitt, J. Identification of coupled degrees of freedom at the interface between sub-structures. *INTER-NOISE and NOISE-CON Congress and Conference Proceedings*. Institute of Noise Control Engineering, 2018. p. 672-680.
[15] van den Bosch, D., van der Seijs, M., de Klerk, D. A, comparison of two source characterisation techniques proposed for standardisation. *SAE International Journal of Advances and Current Practices in Mobility*, 2019, vol. **1**, no 2019-01-1540, p. 1755-1765.
[16] "ISO TC-43 / NWIP 21955 'Vehicles — Experimental method for transposition of dynamic forces generated by an active component from a test bench to a vehicle,'" 2016.
[17] Kohrmann, M., Numerical methods for the vibro-acoustic assessment of timber floor constructions. PhD thesis, Technische Universität München, Germany, 2017.
[18] Klop, R. J., Investigation of hydraulic transmission noise sources. PhD thesis, Purdue University, USA, 2010.